Doppler-Shifted Cyclotron Resonances with Helicons in Copper

S. W. Hui*
School of Physical Sciences, The Flinders University of South Australia, Bedford Park, South Australia
(Received 6 January, 1969)

The nonlocal propagation of helicons in a mixed electron and hole plasma is discussed. The conditions under which the Doppler-shifted cyclotron resonance (DSCR) of either type of carrier are effective are specified. The nonlocal magnetoconductivity, the dispersion relation for helicons, and the consequent surface impedance are evaluated for the case where the helicon wave vector is parallel to **B** and to the [001] axis of copper, assuming Roaf's model of the Fermi surface. The low-rf surface impedance of a copper single crystal of the above orientation is measured at 4.2°K. The standing-wave pattern is damped out before the nonlocal region is reached. The damping effect is interpreted to be the DSCR from the sections of the Fermi surface at $k_{[001]}=0.96$ and 0.60 Å^{-1}. Large surface-impedance anomalies are observed at low field. The field-frequency relation for the surface-impedance anomalies indicates that the electron orbits near the region $k_{[001]}=0.45$ Å^{-1} are responsible. Detailed computation verifies this argument. The result is comparable to that of the magneto-acoustic attenuation measurements.

INTRODUCTION

RECENTLY there were several reports on the measurement of Fermi surfaces by the Doppler-shifted cyclotron resonance (DSCR) with helicons.[1–3] This theory was first suggested, and later developed, by Stern and co-workers.[4,5] In this paper, we present our result and interpretation of helicon measurements in a copper single crystal, with the magnetic field **B** parallel to the [001] axis.

In theory, the DSCR with helicons is very similar to that with ultrasonic shear waves. Both methods draw the same information about the Fermi surface. Detailed magnetoacoustic attenuation experiments on copper single crystals have been reported.[6,7] Their results are comparable to those from our helicon measurements.

1. THEORY

For helicon waves propagating along the magnetic field direction (taken as the z axis of the Cartesian coordinates), the dispersion equation may be written (in mks units), with displacement current neglected, as

$$q^2=i\omega\mu_0\sigma_\pm(q,\omega). \tag{1}$$

Here q and ω are the wave number and angular frequency of the waves, and $\sigma_\pm$ is the conductivity related to the propagation of the circularly polarized waves. The $\pm$ sign indicates left- and right-handed circular polarizations of the waves. In general, $\sigma_\pm$ is a complex quantity, $\sigma_\pm=\sigma'\pm i\sigma''$. The expression for the conductivity $\sigma_\pm$ may be written as[5]

$$\sigma_\pm=\frac{e^2}{4\pi^3 m}\int_{k_-}^{k_+}dk_z\frac{\mathcal{A}(k_z)}{1/\tau+i(\pm\omega_c-\omega-qv_z)}, \tag{2}$$

where k_z is the z component of the electron wave vector, with its extrema at k_+ and k_-. The function $\mathcal{A}(k_z)$ is the cross-sectional area enclosed by the Fermi surface on the $k_z=$ const planes, and v_z is the z component of the Fermi velocity of the electrons. The other symbols have their usual meanings. Under the condition $\omega_c\gg 1/\tau\gg\omega$, the real and imaginary parts of (2) may be separated as[5]

$$\sigma'=\frac{e\epsilon}{4\pi^3 B}\int_{k_-}^{k_+}dk_z\frac{\mathcal{A}(k_z)}{(1-u)^2+\epsilon^2}, \tag{3}$$

$$\sigma''=\frac{e}{4\pi^3 B}\int_{k_-}^{k_+}\frac{(1-u)\mathcal{A}(k_z)}{(1-u)^2+\epsilon^2}, \tag{4}$$

where

$$\epsilon=1/\omega_c\tau$$

and

$$u=qv_z/\omega_c=(q\hbar/2\pi eB)(\partial\mathcal{A}/\partial k_z). \tag{5}$$

The nonlocal region is defined by $ql\gtrsim 1$, where l is the carrier mean free path. DSCR occurs when u approaches unity and $\epsilon\ll 1$. In this case, the denominators of the integrands of σ' and σ'' tend to zero. The onset values of B and q, say, B_0 and q_0, are given by the maximum value of $|\partial\mathcal{A}/\partial k_z|$, as shown in (5). At the onset, the attenuation of the wave increases suddenly, and the dispersion relation is no longer quadratic. There exist more than one solution in (1) for helicons. The degeneracy and attenuation of helicons indicate the onset of DSCR.

The resonance part of the denominators $(1-u)$ selects the band of interacting electrons which constitute the DSCR. The width of the DSCR zone on the Fermi surface is of order ϵ. When ϵ is not much smaller than unity, the zone is wide and the effect of the details of the Fermi surface is smeared out. On the other hand, the value of $|\partial^2\mathcal{A}/\partial k_z^2|$ determines the density of orbits in the DSCR zone. If $|\partial^2\mathcal{A}/\partial k_z^2|$ is very large in the

* Present address: Physics Department, Carnegie-Mellon University, Pittsburgh, Pa.
[1] M. T. Taylor, Phys. Rev. **137**, A1145 (1965).
[2] J. L. Stanford and E. A. Stern, Phys. Rev. **144**, 534 (1966).
[3] J. R. Houck and R. Bowers, Phys. Rev. **166**, 397 (1968).
[4] E. A. Stern, Phys. Rev. Letters **10**, 91 (1963).
[5] J. C. McGroddy, J. L. Stanford, and E. A. Stern, Phys. Rev. **141**, 437 (1966).
[6] J. R. Boyd and J. D. Gavenda, Phys. Rev. **152**, 645 (1966).
[7] M. H. Jericho and A. M. Simpson, Phil. Mag. **17**, 267 (1968).

neighborhood of the maximum of $|\partial \mathcal{A}/\partial k_z|$, the zone may contain too few orbits for its effect to be observed. The "effectiveness" in DSCR is proportional to the number of orbits in the zone; therefore, it is proportional to $(\epsilon|\partial^2\mathcal{A}/\partial k_z^2|_{\mathrm{av}})^{-1}$, where the subscript av indicates the zone-average value. The observable onset of DSCR is then given by the zone having the highest effective value of $|\partial \mathcal{A}/\partial k_z|$ for a particular $\omega_c\tau$ value.

In the case where the Fermi surface consists of both electron and hole zones, the dispersion and the polarization of the waves are determined by the excess of the majority carriers.[8] The resonance condition $u \to 1$ requires the effective $(\partial \mathcal{A}/\partial k_z)$ to bear the same sign as the effective carrier charge. Thus the effective DSCR zone may locate on either the majority or the minority carrier region of the Fermi surface, depending on the sign of the effective $(\partial \mathcal{A}/\partial k_z)$. In the former case, the singular contribution to the σ'' integral is in the same sense as the nonsingular section of the integral; hence there is a sudden increase of σ'' when the resonance condition is met. In the latter case, the singular contribution tends to cancel with the rest of the integral, and results in a sudden decrease of σ'' at resonance. The resonance effect on σ' is invariant to the sign of the effective carrier charge, since the sign of ϵ renders the expression of σ' to be an even function of e. Therefore, σ' always increases at the resonance onset. The physical picture is this. The sense of polarization of the helicons is determined by the charge of the majority carriers. The phase velocity of the helicons is usually several magnitudes lower than the Fermi velocities of the carriers; hence the waves may be regarded as stationary for this purpose. The minority DSCR carriers are those travelling along the static magnetic field direction, so that they see the magnetic field of the wave rotating in the same sense as their cyclotron motion. For the same reason, the majority DSCR carriers are those travelling opposite to the direction of the static magnetic field. These DSCR carriers react with the wave in different manners; thus their effects on the dispersion are the opposite. Yet the absorption of energy from the wave by these DSCR carriers is the same in both cases.

The surface impedance related to helicon propagations is[5]

$$Z=R+iX=\frac{2i\omega\mu_0}{\pi}\int_0^\infty \frac{dq}{q^2+i\omega\mu_0\sigma}. \tag{6}$$

In the local case where $\sigma' \ll \sigma''$ and both are q-independent, (6) may be evaluated by contour integration. There are exactly two poles, one in each half of the complex q plane. The result gives

$$Z=(i\omega\mu_0/\sigma)^{1/2}. \tag{7}$$

In the nonlocal case, σ is a function of q and there is more than one pole in each half-plane. The coincidence of two poles leads to an unremovable singularity, which occurs approximately, but not exactly, at the DSCR edge.[5] This singularity, rather than the edge, gives the anomaly in the surface impedance.[1,9]

2. COMPUTATION

Copper was chosen for investigation because of its relatively well-known Fermi surface.[10] When B is parallel to [001], all cyclotron orbits are closed. If we take the symmetry center Γ of the Brillouin zone to be the origin and take [001] along OZ, the regions $0<|k_z|<0.60$ Å^{-1} and $0.96<|k_z|<1.33$ Å^{-1} are enclosed by electron orbits. Between these regions are the volumes bounded by the so-called four-rosette hole orbits. These volumes are uncompensated. Electrons are the majority carriers, with 0.51 net electrons per atom.[11] Thus, helicons exist and their dispersion relation gives the above "charge density."[12] We have computed from Roaf's parameters[10] the values of $\mathcal{A}(k_z)$ and $(\partial \mathcal{A}/\partial k_z)$. Roaf's results were an empirical fitting of certain experimental data. Recent calculations by Green's-function[13] and augmented-plane-wave methods[14] showed general agreement with Roaf's data, apart from the regions near the neck. As shown below, these regions are comparatively ineffective in DSCR at low values of $\omega_c\tau$. Hence the empirical data are satisfactory for our purpose. The values of $|\partial \mathcal{A}/\partial k_z|$ are shown in Fig. 1. The free-electron values are also shown for comparison.

σ was evaluated by numerically integrating (3) and (4), based on the above data. Since the integrands concern only the areas but not the shapes of the cross sections of the Fermi surface, fine radial features are masked, and the calculation is equivalent to assuming a cylindrically symmetric Fermi surface. The calculation was performed on a CDC 6400 computer. In the com-

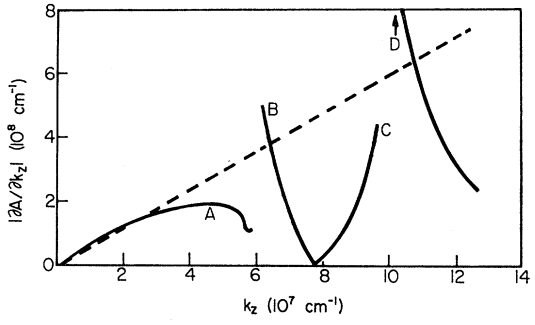

FIG. 1. $|\partial A/\partial k_z|$ for the Fermi surface of copper versus k_z along the [001] axis. The dashed line represents that of a Fermi sphere. The extremes are marked by letters.

[8] We consider only the case where all cyclotron orbits are closed. The open orbit effect is discussed in Ref. 12.

[9] S. W. Hui, J. Sci. Instr. 44, 279 (1967).
[10] D. J. Roaf, Phil. Trans. Roy. Soc. London **A255**, 135 (1962).
[11] J. R. Klauder, W. A. Reed, C. F. Brennert, and J. E. Kunzler, Phys. Rev. **141**, 592 (1966).
[12] S. W. Hui, J. Appl. Phys. (to be published).
[13] J. S. Faulkner, H. L. Davis, and H. W. Joy, Phys. Rev. **161**, 656 (1967).
[14] E. C. Snow, Phys. Rev. **171**, 785 (1968).

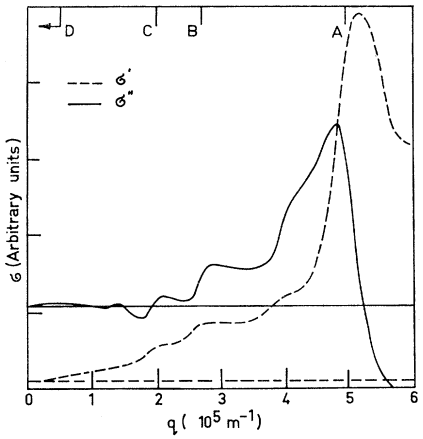

FIG. 2. Real and imaginary parts of σ are plotted as functions of q. $\omega_c\tau=20$. Nonlocal anomalies are generated by the sections of the Fermi surface labelled by the pertinent letters in Fig. 1. Horizontal lines represent local theory.

putation we took Δk_z to be 0.025 Å^{-1}, which was equivalent to taking 53 bands to cover half of the Fermi surface. At the same time, parameters of a hypothetical spherical Fermi surface were integrated by the same program as a check. Because of the rapid variation of $|\partial\mathcal{A}/\partial k_z|$ in the former case and the comparatively coarse grid we took, the singularities were not always shown. The program was thus made to locate the singularity when it existed, and to evaluate it analytically. At the same time the sporadic singular values encountered in the numerical integration were removed. The results of σ' and σ'' are shown in Fig. 2. From the output of intermediate steps of the computation, we located the sections of the Fermi surface which were responsible for the anomalies of the curves. We see that, although the departures from the local results start at quite low q values, caused by the $k_z\sim0.96$ Å^{-1} region of the Fermi surface, the anomaly caused by the $k_z\sim0.45$ Å^{-1} region is by far the most prominant. This is due to the fact that, in this neighborhood, $\partial^2\mathcal{A}/\partial k_z^2\sim0$ and $\partial\mathcal{A}/\partial k_z$ is a slowly varying function covering the largest range in k_z. Thus it is the most effective DSCR zone, and the only significant one when $\omega_c\tau<20$. This is the "finite-orbit-edge" case referred to in Ref. 5. In fact, the DSCR zones at the neck regions where $k_z=\pm0.60$ and ±0.96 Å^{-1} are also in the form of "finite orbit," since the $\mathcal{A}(k_z)$ at these values are nonzero. However, because of the steep slopes of $|\partial\mathcal{A}/\partial k_z|$ at these zones, their influence on σ'' is rather small at finite $\omega_c\tau$. Yet as an accumulative effect, the increase of σ' at these "edges" is significant. This may be seen from the effect on σ' due to the hole sections $k_z=0.60$ and -0.96 Å^{-1}, where slopes are not so steep. Because of the attenuation effect of these zones, the helicons may well be damped out before the most effective onset at $\partial\mathcal{A}/\partial k_z\sim2.0$ Å^{-1} is reached.

The computed data of $\sigma(q)$ were then used to evaluate (6) numerically. The integration over q was cut off at a value 10 times the highest q_0. The poles and their residues were treated by the same manner as in the σ case. We performed the calculations at fixed frequency and varying magnetic field, as used in our experimental procedure. Again, the free-electron case was evaluated for comparison. One example of the computer graph plotter output is shown as the dashed line in Fig. 3. The main peak, shown in Fig. 3 at $B=8.5$ kG, appears at all frequencies. This anomaly was found to be generated by the sections of the Fermi surface where $\partial\mathcal{A}/\partial k_z=2.0$ Å^{-1}. Anomalies generated by other sections having higher $|\partial\mathcal{A}/\partial k_z|_{\max}$ occurred at higher fields and were unresolved at $\tau=5\times10^{-11}$ sec. However, if we knew precisely the values of $(\partial\mathcal{A}/\partial k_z)$ which were likely to cause anomalies, we could calculate, through the dispersion equation, the field-frequency relations of these "anomalies" even if they were unresolved. The field-frequency relations for several of these anomalies were calculated and are presented in Fig. 4. These relations are cubic, in general.[2] In the calculations, the anomalies were assumed to be caused by each of the extreme orbits alone, the effects of neighboring orbits not being taken into account.

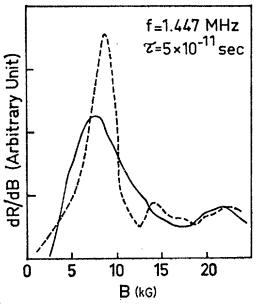

FIG. 3. Example of the variation of the field derivatives of the surface resistance with magnetic field in a copper single crystal; B is parallel to [001]. The excitation frequency is 1.447 MHz. The dashed line is the theoretical curve using $\tau=5\times10^{-11}$ sec.

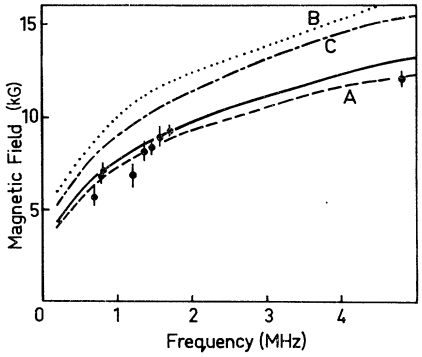

FIG. 4. Magnetic fields of surface-impedance anomalies are plotted against their frequencies. The solid line is computed from the weighted effects of the whole Fermi surface. Points are experimental results. Dashed lines represent the hypothetical anomalies that would have been generated by certain single orbits on the Fermi surface marked by the corresponding letters in Fig. 1.

3. EXPERIMENT

Copper single crystals were grown by Bridgman's method. 99.999% pure copper rods, obtained from Koch

Light & Co., were melted in a graphite crucible placed in an induction furnace. The thermal gradient was provided by a radiation absorber placed near the tapered bottom of the crucible, while the induction furnace was gradually decoupled. The crystal axes were located with x rays in order to orient and spark-cut a thin rectangular plate. The dimensions of the plate used were $8.5\times10.0\times0.245$ mm. When checked again by x rays, the [001] axis was found to be normal to the plate surface. The plate was annealed under 10^{-3} Torr of oxygen for 1 h, and under vacuum for 23 h at 950°C, and was polished chemically afterwards. The residual resistivity ratio was about 2000. Its thickness was measured by a travelling microscope before it was inserted into the sample holder.

The methods used for the surface-impedance measurement have been described elsewhere.[9] Both the oscillator and phase-bridge methods were used. The sample coils were tightly wound on the sample plate. The flat surface of the sample was normal to the axis of a superconducting solenoid. The sample and coils were kept under liquid helium at 4.2°K.

The variations of the impedance of the sample coil were plotted as functions of the magnetic field, for several fixed frequencies ranging between 0.2 and 5 MHz. The detector output was differentiated by an RC circuit while the magnetic field was scanned at a constant rate. An example is shown in Fig. 3. At high fields, (>25 kG), standing-wave resonances were observed. The dispersion relation of the standing waves gave the equivalent charge density of the supporting medium. The result confirmed the calculation of charge densities based on the above model.[12]

In the low-field region where nonlocal effects were expected, we observed a turning point at $B\sim10$ kG, where the slope of the impedance curve changed definitely. This broad transition occurred at all frequencies, except at very low frequencies (≤218 kHz), where this transition appeared at very low field and was hardly visible. These anomalies were similar to those detected in sodium DSCR experiments.[9] The magnetic field values of these anomalies were plotted against the frequencies in Fig. 4. The field values were taken at the peaks of the dR/dB graphs or at the base line crossings of the dX/dB graphs. These positions agreed within experimental error. The poor accuracy was due to the broadness of the transitions.

Unlike the case of sodium,[15] the standing-wave resonance in this experiment obeyed the local dispersion relation until the pattern disappeared at low magnetic field. Even by using a higher excitation frequency to bring up the q_0 to higher magnetic fields, (in order to obtain higher $\omega_c\tau$), we still failed to extend the standing-wave pattern near the anomaly.

[15] S. W. Hui, Phys. Letters **24A**, 265 (1967).

4. INTERPRETATION

There is no simple interpretation of our result, for the following reasons. Firstly, since the value of q_0 is not a measurable quantity, we cannot derive the effective $(\partial\mathcal{A}/\partial k_z)$ directly from Eq. (5). The only way to obtain q_0 is to calculate from the nonlocal dispersion relation, which assumes the knowledge of the Fermi surface. Thus, at most, we arrive at a self-consistency argument. Secondly, the anomalies of the surface impedance do not exactly represent the DSCR onsets.[5] Therefore, (5) must be replaced by (6) in the interpretation of surface-impedance experiments.

After the unavoidable and laborious computation, we obtained theoretical curves for the surface impedance as functions of B. One of these curves is shown in Fig. 3, as is the corresponding experimental curve. The difference in peak height and width is probably due to the difference between the value of τ on the DSCR zone and the average value used in the computation. The difference in the peak position is discussed later. Like the experimental results, there is only one main anomaly shown in each computed curve. This anomaly is caused by the section of the Fermi surface near $k_z=0.46$ Å^{-1}. There are also small "bumps" caused by the hole sections at $k_z=0.60$ and 0.96 Å^{-1} but their effect at finite $\omega_c\tau$ is quite negligible, apart from the accumulative damping effects on the standing-wave resonance. The effect given by the electron section at $k_z=0.96$ Å^{-1} is even smaller and starts at very low q, or, equivalently, at high field.

When the field-versus-frequency relation for the main anomaly is compared with the computed results in Fig. 4, it becomes obvious that the anomaly we observed is the one obtained from computed results. This anomaly is caused mainly by the section of the Fermi surface around $k_z=0.46$ Å^{-1}. The slight displacement of the experimental points towards curve A suggests that certain orbits in the region A weighs more than the average in producing the anomaly. The "cap" at $k_z=1.33$ Å^{-1} has a similar value of $|\partial\mathcal{A}/\partial k_z|$. Yet its contribution to the integrals (3) and (4) is very small, apart from the fact that its $|\partial\mathcal{A}/\partial k_z|$ is a minimum. This main anomaly corresponds to the 110-MHz ultrasonic attenuation peak at $B=4$ kG, since they are caused by the same section of the Fermi surface.[6]

We also suggest that the attenuation, which cuts off the standing-wave pattern well before the edge, is caused by the damping effect from the ends of the hole sections. Unfortunately, with our low $\omega_c\tau$ value, these zones are not effective enough to generate distinct surface-impedance anomalies. The damping alone provides no quantitative proof to this assumption. However, with a very pure sample, we wish to observe and resolve the anomalies presumably caused by these regions near the necks. Here one needs to study the geometry of the neck regions in detail. The observed, but yet unexplained, ultrasonic absorption peaks between 3 and 10 kG at 100 MHz may also be caused by these regions.[7]

The proper identification of these peaks would substantiate our theory of minority carrier DSCR.

ACKNOWLEDGMENTS

The author wishes to thank A. L. Francey, Dr. D. J. Roaf, Dr. D. A. Smith, and Dr. B. Davies for valuable discussions. The communication with Professor E. A. Stern is appreciated. The experimental work was performed at the Physics Department of Monash University under the Monash University Research Grant. The computations were done at the University of Adelaide Computing Center.

PHYSICAL REVIEW VOLUME 185, NUMBER 3 15 SEPTEMBER 1969

Magnetothermal Oscillations and the Fermi Surface of ReO_3

J. E. GRAEBNER AND E. S. GREINER
Bell Telephone Laboratories, Murray Hill, New Jersey 07974
(Received 3 April 1969)

Magnetothermal oscillations have been observed in single crystals of ReO_3. The three sets of frequencies observed are in good agreement with Mattheiss's augmented-plane-wave calculations, which include open orbits along ⟨100⟩ directions.

I. INTRODUCTION

THE compound ReO_3 is a red transition-metal oxide which exhibits metallic electrical conductivity. In addition to its importance as a transition-metal oxide,[1] ReO_3 is interesting because of its relatively simple crystal structure. This structure makes it closely related to certain classes of materials of wide current interest: the perovskites and the tungsten bronzes. As such it serves as a prototype for understanding the electronic band structure of these more complicated materials.

Detailed band-structure calculations using the augmented-plane-wave (APW) method have recently been completed by Mattheiss.[2] Optical data have been reported by Feinleib *et al.*[3] and de Haas–van Alphen (dHvA) data have been reported by Marcus.[4] The optical data, as well as the lowest dHvA frequency and its effective mass, were used by Mattheiss to adjust the band-structure calculations.

Magnetothermal oscillations[5] are the Landau quantum oscillations in the temperature of an adiabatically isolated sample as the magnetic field is changed in magnitude or direction. We present here detailed data which combine rotations and field sweeps to determine precisely the frequencies and their dependence on magnetic-field direction. The dHvA data[4] were obtained at lower fields and did not include rotation data. They are roughly consistent with the present data, but the large scatter precludes any detailed comparison with the present results.

II. THEORY

The ReO_3 structure has a simple cubic Bravais lattice and is illustrated in Fig. 1. The cube corner positions are unoccupied in ReO_3 but are occupied by A atoms in the perovskite structure ABO_3, or by Na atoms in sodium tungsten bronze, Na_xWO_3.

The APW Fermi surface is illustrated in Fig. 2. The two smallest pieces, α and β, are roughly spherical and centered at Γ. The third piece γ consists of ⟨100⟩-directed cylinders intersecting at Γ and forming in the extended zone scheme a jungle-gym-like multiply connected surface. Electron orbit γ_1 and hole orbit γ_2 are illustrated in the figure. Electron orbit γ_3 is not

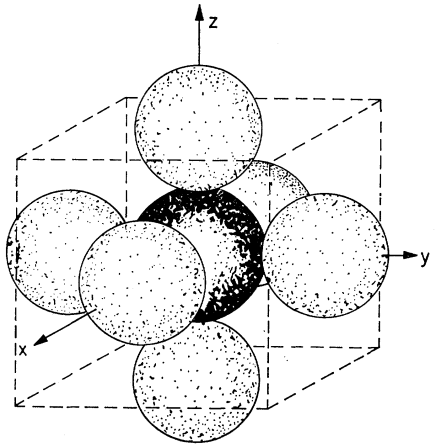

FIG. 1. Unit cell for ReO_3. The rhenium atom at the center of the cube is surrounded by six oxygen atoms located at the face centers (after Mattheiss).

[1] For a review of the transition metal oxides and their many interesting properties, see David Adler, in *Solid State Physics*, edited by F. Seitz, D. Turnbull, and H. Ehrenreich (Academic Press Inc., New York, 1968), p. 1, and references therein.
[2] L. F. Mattheiss, Phys. Rev. **181**, 987 (1969).
[3] J. Feinleib, W. J. Scouler, and A. Ferretti, Phys. Rev. **165**, 765 (1968).
[4] S. M. Marcus, Phys. Letters **27A**, 584 (1968).
[5] J. E. Kunzler, F. S. L. Hsu, and W. S. Boyle, Phys. Rev. **128**, 1084 (1962).